Pergamon

Int. J. Heat Mass Transfer. Vol. 41, No. 3, pp. 547–562, 1998

Printed in Great Britain
0017–9310/98 $19.00+0.00

PII: S0017–9310(97)00189–0

Unsteady natural convection of a dusty fluid in an infinite rectangular channel

D. C. DALAL†
Physics and Applied Mathematics Unit, Indian Statistical Institute, 203, B.T.Road, Calcutta 700 035, India

N. DATTA
Department of Mathematics, Indian Institute of Technology, Kharagpur 721 302, India

and

S. K. MUKHERJEA
Department of Applied Mechanics, Bengal Engineering College (Deemed University), Howrah 711 103, India

(*Received* 12 *July* 1995 *and in final form* 23 *May* 1997)

Abstract—Natural convection of a dusty fluid in an infinite rectangular channel with differentially heated vertical walls and adiabatic horizontal walls has been studied. The problem has been solved using a combination scheme of central and second upwind differencing. It is seen that the heat transfer rate decreases with an increase of mass concentration of dust particles, but it increases with an increase of the Rayleigh number. © 1997 Elsevier Science Ltd.

1. INTRODUCTION

There have been numerous theoretical and experimental studies of heat and mass transfer induced by natural convection in fluids. These studies have many applications in physical systems where heat transport by buoyancy induced convective motion takes place, such as, chemical reactor, nuclear reactor, combustion systems, pneumatic transport etc. In some of these applications, the fluid may contain suspended dust particles.

Kazakevich and Kravipin [1] have experimentally studied the aerodynamic resistance of a dusty gas flowing through a system of pipes and have shown that the resistance is less than that of the clear gas. Saffman [2] gave a model for theoretical investigation of the above phenomenon. Saffman found an explanation of reduction of viscosity in that the dust particles in any gas have much larger inertia than that the equivalent volume of air. The relative motion of the dust particles and the air will dissipate energy because of the drag between dust and air, and thus energy is extracted from the system. Saffman verified the above hypothesis on studying the stability of a laminar flow by investigating the effects of dust particles on the critical Reynolds number for transition to turbulent flow. Marble [3] extended the model of Saffman so as to include slip stress tensor and slip energy flux which arise from momentum transport due to particle motion at velocities different from the mean particle velocity, and different temperature lags within the same region, respectively. In the discussion of Marble's study [3] Hoglund has given a comparison of experimental and theoretical results of gas and particle temperature in a rocket nozzle and remarked that "The important point is that these preliminary data shown calculated and experimental thermal lags in excellent agreement. The closed agreement lends quantitative support to the type of calculations discussed by Marble and, especially, to the accuracy of predictions of particle lag in rocket nozzles."

Farbar and Morley [4] made an experimental study of heat transfer by adding alumina-silica catalyst with air and found that the heat transfer coefficient of the mixture increased. Farbar and Depew [5] studied the effect of the size of dust particles on the rate of heat transfer and showed that it is strongly dependent on the particle size. Sukomel *et al.* [6] performed an experiment to find the rate of heat transfer in the flow of helium, nitrogen and air having suspended particles of graphite and aluminium. It was observed that the rate of heat transfer reduces due to addition of particles if the loading ratio between solid and gas is less than 3. Tien and Quan [7] found that Nusselt number of air with lead is less than that of fresh air and it is significantly lower when glass particles are added to the air. Depew and Kramer [8] made a critical review on heat transfer to flowing gas–solid mixtures. They

† Present address: Department of Mathematics, Indian Institute of Technology Guwahati, Institution of Engineers Building, Panbazar, Guwahati 781 001, Assam, India.

NOMENCLATURE

A	aspect ratio (l/d_c)
c_p	specific heat of fluid
c_s	specific heat of particle phase
$\mathbf{D}$	divergence of velocity vector
d_c	width of the channel
d_p	work done by the particle phase per unit volume
f	mass concentration of particle phase
$\mathbf{F}_b$	body force on fluid per unit volume
$\mathbf{F}_p$	fluid-particle interaction force per unit volume
$\boldsymbol{g}$	acceleration due to gravity
k	thermal conductivity of fluid
l	height of the channel
m	mass of a particle
N	number density of particles
p	pressure of fluid
p_s	static pressure of fluid
$\mathbf{q}$	velocity vector of fluid
q_f	rate of heat flux of fluid
q_s	rate of heat flux of particle phase
Q_p	thermal interaction force per unit volume
r_p	radius of particle
t	time
T	temperature of fluid
T_i	initial temperature
u	x-component velocity of fluid
v	y-component velocity of fluid
x, y, z	Cartesian coordinates.

Greek symbols

α_c	combination factor
α_d	dust parameter
β	coefficient of thermal expansion
γ	ratio of c_s and c_p
δt	increment of time
δx	increment of x
δy	increment of y
ΔT	temperature difference
ζ	vorticity of fluid
μ	coefficient of viscosity of fluid
ν	kinematic viscosity of fluid
ρ	density of fluid
τ_m	velocity relaxation time of particles
τ_T	thermal relaxation time of particles
ϕ_{u_R}	momentum flux of u_R
ψ	stream function.

Subscripts

B	value at bottom face of control volume
ij	value at (i,j) cell
L	value at left face of control volume
M	value at the middle of the channel
p	for particle phase
R	value at right face of control volume
T	value at top face of control volume
W	value at the wall of the channel.

Superscripts

n	value at nth time step
*	for dimensionless value.

have discussed experimental as well as theoretical study. Tien [9] derived the energy relationships and produced a set of equations which are very similar to Saffman's model. Performing an experiment on the transportation of glass particles in air through a tube having uniform heat flux, Depew showed that these equations are valid for 30 mμ spheres and Reynolds number ($<30\,000$). In their review they concluded that data collected by various investigators indicate that heat transfer can be augmented by the addition of solid particles to a gas stream. The results are applicable only to very dilute concentrations and to very small particles which follows Stokes' drag law. They have shown that under these conditions there are good agreement between the results obtained from experimental and the above model.

Ramamurthy [10] studied the free convection effects on the Stokes problem for an infinite vertical plate in a dusty fluid analytically and showed that the rate of heat transfer is directly proportional to mass concentration of particles. However, not many studies on natural convection problem of dusty fluid are reported in available literature.

Investigations on the natural convection of clear fluid in a rectangular cavity for transient heating of the vertical walls have been made by several authors. The aspect ratio (A) of the cavity or channel, defined by the ratio of the height of the channel to its width, plays an important role in the convection phenomenon. Batchelor [11], Poots [12] and Gill [13] found analytical solution, whereas Wilkes and Churchill [14] and De Vahl Davis [15] solved the problem numerically when $A \geqslant 1$. For rectangular cavity with aspect ratio $A \leqslant 1$, Patterson and Imberger [16] have given a numerical solution. They have shown that a number of initial flow types are possible which ultimately leads to two basic types of steady flow determined by the relative values of the dimensionless parameters, e.g. Prandtl number, Rayleigh number describing the flow.

In the present study, free convective heat transfer to a dusty fluid due to differentially heated vertical walls of a rectangular channel has been considered.

The governing equations for the two-dimensional convective flow are coupled and non-linear, hence, it is not possible to get an analytical solution. This problem has been solved by finite difference method using staggered grid.

2. FORMULATION OF THE PROBLEM

We consider a dusty fluid initially at rest within an infinitely long closed rectangular horizontal channel. We have taken z-axis along the axis of the channel, x-axis vertically upwards and y-axis horizontally, but perpendicular to the axis of the channel as shown in Fig. 1. Let the height and width of the channel be l and d_c, respectively. Initially, the system is having a uniform temperature T_i. Suddenly, the wall $y = 0$ is heated to a temperature $T_i + \Delta T$ and the wall $y = d_c$ is cooled to a temperature $T_i - \Delta T$ and natural convection starts due to this.

Following Saffman's model [2] of a dusty fluid, the governing equations for two-dimensional incompressible flow given by Marble [3] is

$$\operatorname{div} \cdot \mathbf{q} = 0 \tag{1}$$

$$\rho \left\{ \frac{\partial \mathbf{q}}{\partial t} + (\mathbf{q} \cdot \nabla)\mathbf{q} \right\} = -\nabla p + \nabla(\mu \nabla \cdot \mathbf{q}) + \mathbf{F}_p + \mathbf{F}_b \tag{2}$$

$$\rho c_p \left\{ \frac{\partial T}{\partial t} + (\mathbf{q} \cdot \nabla) T \right\} = q_f + Q_p + d_p + \Phi_f \tag{3}$$

$$\operatorname{div} \cdot \mathbf{q}_p = 0 \tag{4}$$

$$\rho \left\{ \frac{\partial \mathbf{q}_p}{\partial t} + (q_p \cdot \nabla)\mathbf{q}_p \right\} = -\nabla p_p - \mathbf{F}_p + \mathbf{F}_{bp} \tag{5}$$

$$\rho c_s \left\{ \frac{\partial T_p}{\partial t} + (\mathbf{q}_p \cdot \nabla) T_p \right\} = q_s - Q_p \tag{6}$$

where the volume fraction and viscosity of the pseudo-fluid of solid particles have been neglected. Here $\mathbf{q}$, T, p, $\mathbf{F}_b$ and ρ are velocity, temperature, pressure, body force and density of fluid, respectively, and a subscript p in them denotes corresponding entities of particle phase. μ and c_p, respectively, are the viscosity and specific heat of fluid. c_s is the specific heat of particles. q_f and q_s, represent heat fluxes for fluid and for particle phase, respectively. Φ_f is the viscous dissipation of fluid. $\mathbf{F}_p$ is the total fluid–particle interaction force per unit volume. If Reynolds number based on the relative velocity of particle is less than unity then the force accelerating the particle to the fluid speed is given by Stokes law which is $6\pi r_p \mu(\mathbf{q}_p - \mathbf{q})$, where r_p is the radius of a particle. If N is assumed to be the number density of particles, the total interaction force per unit volume is

$$\mathbf{F}_p = 6\pi N r_p \mu(\mathbf{q}_p - \mathbf{q}) = \rho_p(\mathbf{q}_p - \mathbf{q})/\tau_m$$

$\tau_m = m/6\pi\mu r_p$; is called relaxation time during which the velocity of the particle phase relative to the fluid is reduced to $1/e$ times its initial value and m is the mass of each particle. Similarly, the total thermal interaction between the fluid and particle phase per unit volume is given by

$$Q_p = \rho c_s(T_p - T)/\tau_T$$

and $\tau_T = mc_s/4\pi k r_p$ is thermal relaxation time of particle phase, i.e. time τ_T, the temperature of the particle phase relative to the fluid is $1/e$ times the initial value. The rate of work done by the particles due to the force of interaction with the fluid is

$$d_p = (\mathbf{q}_p - \mathbf{q}) \cdot \mathbf{F}_p.$$

In most of the studies of dusty fluid flows, certain

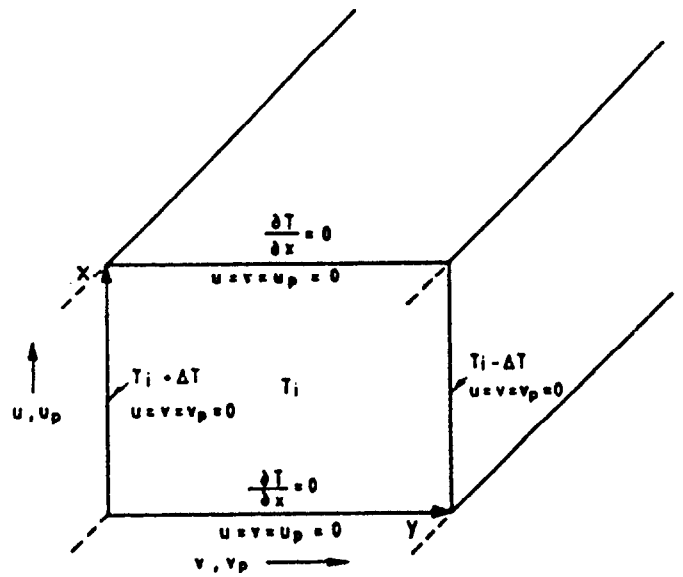

Fig. 1. Schematic diagram of the cross-section of an infinite rectangular channel.

simplifying assumptions are usually made for dilute suspensions. In this study the following assumptions have been made:

(1) The number density N of particles is constant.
(2) The solid particles are sparsely distributed and they are non-interacting, so that the pressure locally have same velocity vector and temperature. Due to this assumption of lack of randomness in local particle motion, the pressure associated with the particle cloud is negligible. Then the fluid pressure p will be the same as the total pressure of the mixture.

The temperature difference between two vertical walls is considered to be small so that the change in viscosity is not significant and the flow can be assumed as laminar. Assuming all external forces other than gravitational forces to be negligible, the governing equations for two-dimensional free convective flow can be written, from above equations, as

$$\frac{\partial u}{\partial x}+\frac{\partial v}{\partial y}=0 \tag{7}$$

$$\rho\left(\frac{\partial u}{\partial t}+u\frac{\partial u}{\partial x}+v\frac{\partial u}{\partial y}\right)=-\frac{\partial p}{\partial x}+\mu\left(\frac{\partial^2 u}{\partial x^2}+\frac{\partial^2 u}{\partial y^2}\right)+\frac{\rho_p}{\tau_m}(u_p-u)-g\rho \tag{8}$$

$$\rho\left(\frac{\partial v}{\partial t}+u\frac{\partial v}{\partial x}+v\frac{\partial v}{\partial y}\right)=-\frac{\partial p}{\partial y}+\mu\left(\frac{\partial^2 v}{\partial x^2}+\frac{\partial^2 v}{\partial y^2}\right)+\frac{\rho_p}{\tau_m}(v_p-v) \tag{9}$$

$$\rho c_p\left(\frac{\partial T}{\partial t}+u\frac{\partial T}{\partial x}+v\frac{\partial T}{\partial y}\right)=k\left(\frac{\partial^2 T}{\partial x^2}+\frac{\partial^2 T}{\partial y^2}\right)+\frac{\rho_p c_s}{\tau_T}(T_p-T)+\frac{\rho_p}{\tau_m}\{(u_p-u)^2+(v_p-v)^2\} \tag{10}$$

$$\frac{\partial u_p}{\partial x}+\frac{\partial v_p}{\partial y}=0 \tag{11}$$

$$\rho_p\left(\frac{\partial u_p}{\partial t}+u_p\frac{\partial u_p}{\partial x}+v_p\frac{\partial u_p}{\partial y}\right)=-\frac{\rho_p}{\tau_m}(u_p-u) \tag{12}$$

$$\rho_p\left(\frac{\partial v_p}{\partial t}+u_p\frac{\partial v_p}{\partial x}+v_p\frac{\partial v_p}{\partial y}\right)=-\frac{\rho_p}{\tau_m}(v_p-v) \tag{13}$$

$$\rho_p c_s\left(\frac{\partial T_p}{\partial t}+u_p\frac{\partial T_p}{\partial x}+v_p\frac{\partial T_p}{\partial y}\right)=-\frac{\rho_p c_s}{\tau_T}(T_p-T) \tag{14}$$

where u, v are the velocity components along x- and y-axis.

Initially, the dusty fluid is considered to be at rest and the convection starts by sudden change in temperature of the vertical walls. Actually this initial condition seems to be unrealistic, but a uniform distribution of suspended particles in a static fluid can be thought for a moment and that moment can be considered to be initial time.

Then the initial conditions are

$$u=v=u_p=v_p=0,$$
$$T=T_p=T_i \quad \text{at } t\leqslant 0, \quad \forall x,y. \tag{15}$$

The temperature of the vertical walls $y=0$ and $y=d_c$ are maintained at $T_i+\Delta T$ and $T_i-\Delta T$, respectively. The boundary conditions at the vertical walls are

$$\left.\begin{aligned} u=v=v_p=0, \quad T=T_i+\Delta T \quad \text{at } y=0\\ u=v=v_p=0, \quad T=T_i-\Delta T \quad \text{at } y=d_c\end{aligned}\right\}\forall x. \tag{16}$$

The horizontal walls are insulated and thus the boundary conditions at these walls are

$$u=v=u_p=0,$$
$$\frac{\partial T}{\partial x}=0 \quad \text{at } x=0 \quad \text{and at} \quad x=l\,\forall y. \tag{17}$$

To make the above system dimensionless, we introduce the following non-dimensional variables

$$x^*=\frac{x}{d_c},$$
$$y^*=\frac{y}{d_c}, \quad u^*=\frac{ud_c}{\nu}, \quad u_p^*=\frac{u_p d_c}{\nu}$$
$$t^*=\frac{kt}{\rho c_p d_c^2}, \quad v^*=\frac{vd_c}{\nu}, \quad v_p^*=\frac{v_p d_c}{\nu}$$
$$p^*=\frac{(p-p_s)d_c^2}{\rho\nu^2}, \quad T^*=\frac{T-T_i}{\Delta T}, \quad T_p^*=\frac{T_p-T_i}{\Delta T}.$$

Here p_s, ν are the static pressure and kinematic viscosity of fluid.

Incorporating Boussinesq approximation in equation (8) and using the above non-dimensional variables, the dimensionless form of the equations (7)–(15) can be written in conservative form, on dropping asterisks, as

$$\frac{\partial u}{\partial x}+\frac{\partial v}{\partial y}=0 \tag{18}$$

$$\frac{1}{Pr}\frac{\partial u}{\partial t}+\frac{\partial u^2}{\partial x}+\frac{\partial uv}{\partial y}=-\frac{\partial p}{\partial x}+\frac{\partial^2 u}{\partial x^2}+\frac{\partial^2 u}{\partial y^2}+f\alpha_d(u_p-u)+GT \tag{19}$$

$$\frac{1}{Pr}\frac{\partial v}{\partial t}+\frac{\partial uv}{\partial x}+\frac{\partial v^2}{\partial y}=-\frac{\partial p}{\partial y}+\frac{\partial^2 v}{\partial x^2}+\frac{\partial^2 v}{\partial y^2}+f\alpha_d(v_p-v) \tag{20}$$

$$\frac{1}{Pr}\frac{\partial T}{\partial t}+\frac{\partial uT}{\partial x}+\frac{\partial vT}{\partial y}=\frac{1}{Pr}\left(\frac{\partial^2 T}{\partial x^2}+\frac{\partial^2 T}{\partial y^2}\right)$$

$$+\frac{2f\alpha_d}{3Pr}(T_p-T)+f\alpha_d Ec\{(u_p-u)^2+(v_p-v)^2\} \quad (21)$$

$$\frac{\partial u_p}{\partial x}+\frac{\partial v_p}{\partial y}=0 \quad (22)$$

$$\frac{1}{Pr}\frac{\partial u_p}{\partial t}+\frac{\partial u_p^2}{\partial x}+\frac{\partial u_p v_p}{\partial y}=-\alpha_d(u_p-u) \quad (23)$$

$$\frac{1}{Pr}\frac{\partial v_p}{\partial t}+\frac{\partial u_p v_p}{\partial x}+\frac{\partial v_p^2}{\partial y}=-\alpha_d(v_p-v) \quad (24)$$

$$\frac{1}{Pr}\frac{\partial T_p}{\partial t}+\frac{\partial u_p T_p}{\partial x}+\frac{\partial v_p T_p}{\partial y}=-\frac{2\alpha_d}{3\gamma Pr}(T_p-T) \quad (25)$$

where the dimensionless parameters appearing in the above equations are

$$G=\frac{d_c^3 g\beta\Delta T}{\nu^2},$$

$$Pr=\frac{\mu c_p}{k},\quad f=\frac{\rho_p}{\rho},\quad \gamma=\frac{c_s}{c_p}$$

$$Ec=\frac{\nu^2}{d_c^2 c_p\Delta T},\quad \alpha_d=\frac{d_c^2}{\nu\tau_m},\quad \tau_T=\frac{3Pr\gamma\tau_m}{2}.$$

The governing equations have been made dimensionless in such a way so that the equations are free from Reynolds number, but the flow status can be predicted from the values of Rayleigh number ($Ra = Pr*G$).

The dimensionless initial and boundary conditions corresponding to equations (15)–(17) are

$$u=v=u_p=v_p=0,\quad T=T_p=0 \quad \text{at } t\leqslant 0,\quad \forall x,y \quad (26)$$

$$\left.\begin{aligned} u=v=v_p=0,\quad T=1 \quad &\text{at } y=0\\ u=v=v_p=0,\quad T=-1 \quad &\text{at } y=1\end{aligned}\right\}\forall x \quad (27)$$

$$u=v=u_p=0,$$

$$\frac{\partial T}{\partial x}=0 \quad \text{at } x=0 \quad \text{and at} \quad x=A\forall y \quad (28)$$

where $A = l/d_c$.

3. NUMERICAL PROCEDURE

In order to solve the system of equations (18)–(25) under the boundary conditions (27) and (28) numerically, a control volume based finite difference technique with staggered grid has been employed.

Mukherjea [17] has developed a combination scheme in which he has calculated the initial value of pressure from the pressure Poisson equation like MAC method [18] and then used the pressure correction technique of SOLA [19]. He has also used a combination of central and second upwind differencing method for discretization of convective terms. He has shown that this is a faster and more accurate scheme (in terms of flow divergence) than MAC or SOLA. Using staggered grid idea, multiphase flow problems have been solved by Harlow and Amsden [20], and by Di Giacinto [21].

In the present study, neither phase change nor sedimentation has been considered and the volume fraction of the dust particles has been neglected. This problem has been solved using the combination scheme of Mukherjea [17] for fluid phase and SOLA scheme for the particle phase. Primitive variables have been used for computation for fluid phase and then vorticity has been considered for the particle phase. The values of the primitive variables of the particle phase have then been computed using successive over relaxation (SOR) method. The computation has been terminated when the steady state condition is reached.

3.1. *Discretization of the equations*

The cross-section of the channel (shown in Fig. 1) has been considered as the computational domain where x-axis has been taken vertically upward, i.e. in the direction of u and u_p and y-axis horizontally rightward, i.e. in the direction of v and v_p. The increment along x-axis is δx and that along y-axis is δy. The time increment is δt. In this study a uniform grid has been considered.

The value of u at (i,j) cell and at nth time step, usually denoted by u_{ij}^n, has been written as u_{ij}, on dropping the superscript, for convenience. Same convention has been used for other variables also.

The discretized forms of the equations (18)–(21) for a typical cell (i,j) are as follows:

$$\frac{u_{ij}-u_{i-1j}}{\delta x}+\frac{v_{ij}-v_{ij-1}}{\delta y}=0 \quad (29)$$

$$\frac{1}{Pr}\frac{u_{ij}^{n+1}-u_{ij}}{\delta t}=-\frac{p_{i+1j}-p_{ij}}{\delta x}$$
$$+\frac{u_{i+1j}-2u_{ij}+u_{i-1j}}{\delta x^2}+\frac{u_{ij+1}-2u_{ij}+u_{ij-1}}{\delta y^2}$$
$$+f\alpha_d(u_{pij}-u_{ij})+G\frac{T_{i+1j}+T_{ij}}{2}$$
$$-(1-\alpha_c)\frac{u_T u_T-u_B u_B}{\delta x}-\alpha_c\frac{u_T\phi_{u_T}-u_B\phi_{u_B}}{\delta x}$$
$$-(1-\alpha_c)\frac{v_R u_R-v_L u_L}{\delta y}-\alpha_c\frac{v_R\phi_{u_R}-v_L\phi_{u_L}}{\delta y} \quad (30)$$

$$\frac{1}{Pr}\frac{v_{ij}^{n+1}-v_{ij}}{\delta t}=-\frac{p_{ij+1}-p_{ij}}{\delta y}+\frac{v_{i+1j}-2v_{ij}+v_{i-1j}}{\delta x^2}$$
$$+\frac{v_{ij+1}-2v_{ij}+v_{ij-1}}{\delta y^2}+f\alpha_d(v_{pij}-v_{ij})$$
$$-(1-\alpha_c)\frac{u_T v_T-u_B v_B}{\delta x}-\alpha_c\frac{u_T\phi_{v_T}-u_B\phi_{v_B}}{\delta x}$$
$$-(1-\alpha_c)\frac{v_R v_R-v_L v_L}{\delta y}-\alpha_c\frac{v_R\phi_{v_R}-v_L\phi_{v_L}}{\delta y} \quad (31)$$

$$\frac{T_{ij}^{n+1}-T_{ij}}{Pr\,\delta t}$$

$$=\frac{1}{Pr}\left\{\frac{T_{i+1j}-2T_{ij}+T_{i-1j}}{\delta x^2}+\frac{T_{ij+1}-2T_{ij}+T_{ij-1}}{\delta y^2}\right\}$$

$$+f\alpha_d Ec\left\{\left(\frac{u_{pij}+u_{pi-1j}-u_{ij}-u_{i-1j}}{2}\right)^2\right.$$

$$\left.+\left(\frac{v_{pij}+v_{pij-1}-v_{ij}-v_{ij-1}}{2}\right)^2\right\}+\frac{2f\alpha_d}{3Pr}(T_{pij}-T_{ij})$$

$$-(1-\alpha_c)\frac{u_T T_T-u_B T_B}{\delta x}-\alpha_c\frac{u_T\phi_{T_T}-u_B\phi_{T_B}}{\delta x}$$

$$-(1-\alpha_c)\frac{v_R T_R-v_L T_L}{\delta y}-\alpha_c\frac{v_R\phi_{T_R}-v_L\phi_{T_L}}{\delta y} \qquad (32)$$

where ϕ stands for momentum flux and the suffixes B, T, R, L denote the values of the variables at mid point of the bottom, top, right and left faces of control volume, as shown in Fig. 2(a–c).

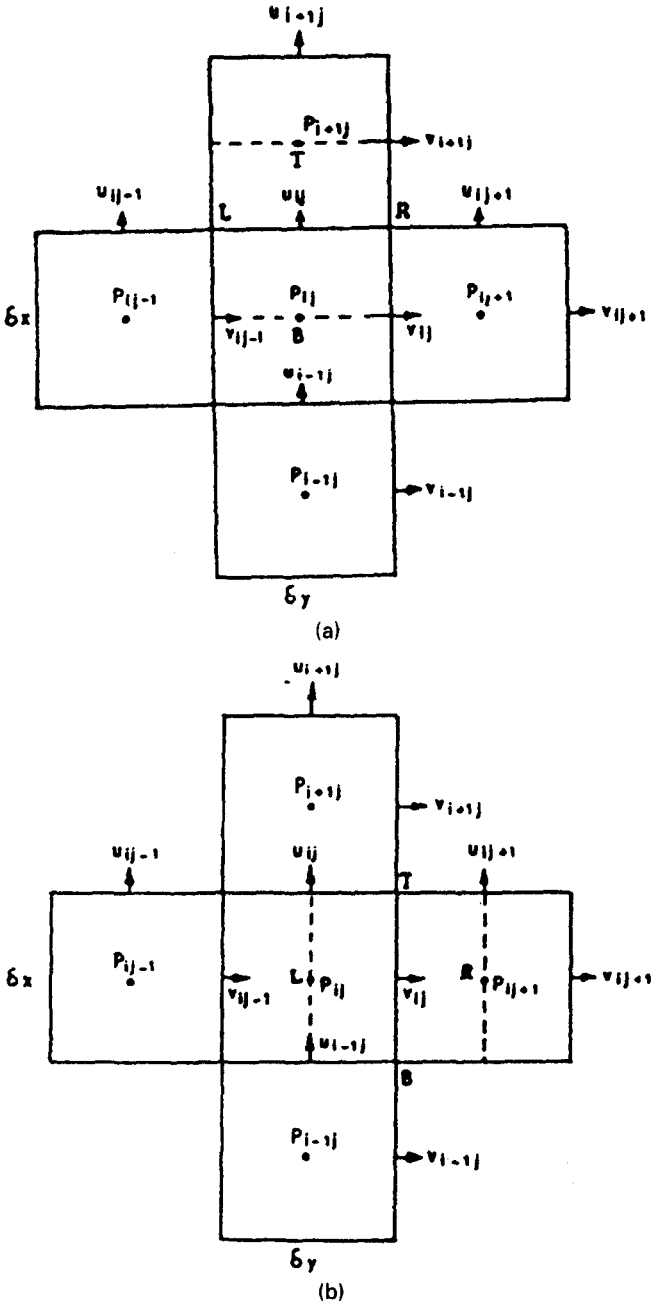

Fig. 2. (a) Control volume for u-momentum of fluid; (b) control volume for v-momentum of fluid; (c) control volume for temperature of fluid.

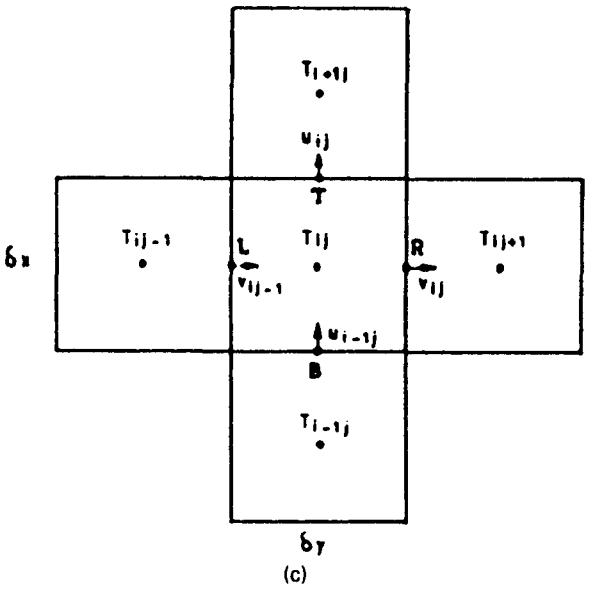

(c)

Fig. 2—*continued.*

From the equation of continuity (22) for particle phase, stream function ψ_p can be introduced as:

$$u_p = -\frac{\partial \psi_p}{\partial y}, \quad v_p = \frac{\partial \psi_p}{\partial x}.$$

Differentiating equations (23) and (24) with respect to y and x, respectively, and subtracting we get:

$$\frac{1}{Pr}\frac{\partial \zeta_p}{\partial t} + \frac{\partial}{\partial x}(u_p \zeta_p) + \frac{\partial}{\partial y}(v_p \zeta_p) = -\alpha_d(\zeta_p - \zeta) \qquad (33)$$

where

$$\zeta_p = \nabla^2 \psi_p = \frac{\partial v_p}{\partial x} - \frac{\partial u_p}{\partial y}$$

is vorticity of the particle phase.

The discretized form of this equation and equation (25) can be written as,

$$\frac{\zeta_{pij}^{n+1} - \zeta_{pij}}{Pr\,\delta t} = -\alpha_d(\zeta_{pij} - \zeta_{ij}) - (1-\alpha_c)\frac{u_{pT}\zeta_{pT} - u_{pB}\zeta_{pB}}{\delta x}$$
$$-\alpha_c \frac{u_{pT}\phi_{\zeta_{pT}} - u_{pE}\phi_{\zeta_{pB}}}{\delta x} - (1-\alpha_c)\frac{v_{pR}\zeta_{pR} - v_{pL}\zeta_{pL}}{\delta y}$$
$$-\alpha_c \frac{v_{pR}\phi_{\zeta_{pR}} - v_{pL}\phi_{\zeta_{pL}}}{\delta y} \qquad (34)$$

$$\frac{T_{pij}^{n+1} - T_{pij}}{Pr\,\delta t} = -\frac{2\alpha_d}{3\gamma Pr}(T_{pij} - T_{ij})$$
$$-(1-\alpha_c)\frac{u_{pT}T_{pT} - u_{pB}T_{pB}}{\delta x} - \alpha_c \frac{u_{pT}\phi_{T_{pT}} - u_{pB}\phi_{T_{pB}}}{\delta x}$$
$$-(1-\alpha_c)\frac{v_{pR}T_{pR} - v_{pL}T_{pL}}{\delta y} - \alpha_c \frac{v_{pR}\phi_{T_{pR}} - v_{pL}\phi_{T_{pL}}}{\delta y} \qquad (35)$$

where $\phi_{\zeta_{pT}}$ etc. denote the velocity flux of the particle phase at point T.

The pressure Poisson equation can be derived by combining the discretized form of continuity and momentum equations as,

$$\frac{p_{i+1j} - 2p_{ij} + p_{i-1j}}{\delta x^2} + \frac{p_{ij+1} - 2p_{ij} + p_{ij-1}}{\delta y^2}$$
$$= \frac{D_{ij}}{\delta t} + \frac{ud_{ij} - ud_{i-1j}}{\delta x} + \frac{vd_{ij} - vd_{ij-1}}{\delta y}. \qquad (36)$$

The details of the discretization has been discussed in the Ph.D. thesis of Dalal [22].

3.2. *Boundary conditions*

The Eulerian cells have been taken in such a way that the solid boundaries coincide with their walls. As a result the normal velocity mesh points always pass through the boundaries. The idea of boundary condition used in MAC formulation by Harlow and Welch [18] has been followed in the present investigation. As the boundary is impermeable, for no-slip, the tangential and normal components of velocity at the boundary have been taken to be zero while for free-slip, only the normal component of velocity has been considered to be zero. The particle phase has been assumed as pseudo-fluid. So particles may slip at the boundary, as a result the tangential components of velocity of particle phase will not be zero, but the normal component of that has been considered to be zero. The stream function of particle phase at solid boundary has been assumed to be zero.

3.3. *Numerical stability*

In order to stabilize the scheme certain restrictions are to be made in mesh sizes δx, δy and time increment

δt. The combination factor is also determined by some restrictions. From CFL (Courant–Friedrich–Lewy) condition [23] it can be considered that the material cannot move through more than one cell in one time step. So δt must satisfy the condition:

$$\delta t \leqslant \frac{1}{Pr}\left[\frac{\delta x}{u}, \frac{\delta y}{v}, \frac{\delta x}{u_p}, \frac{\delta y}{v_p}\right]_{\min}.$$

Here, minimum is in the global sense. Now δt is taken as one-fourth of that found from the above inequality.

From linear stability analysis, considering that the momentum must not diffuse more than one cell in one time step, it can be written that

$$\delta t < \frac{1}{2Pr}\frac{\delta x^2 \delta y^2}{\delta x^2 + \delta y^2}.$$

Finally, we choose a δt which is minimum of the above two values of δt. The combination factor α_c is required to be found properly to ensure the stability. The value is chosen from the inequality,

$$1 \geqslant \alpha_c > \left[\left|\frac{Pru\delta t}{\delta x}\right|, \left|\frac{Prv\delta t}{\delta y}\right|, \left|\frac{Pru_p\delta t}{\delta x}\right|, \left|\frac{Prv_p\delta t}{\delta y}\right|\right]_{\max}.$$

3.4. *Steady-state condition*

Steady state condition has been defined as a state when the average Nusselt number of fluid (Nu) is nearly constant along the horizontal axis. Nu has been calculated at the hotter wall $y = 0$ and that at the middle of the channel, i.e. $y = 0.5$ and checked for equality to find the steady state because there is symmetry in the flow and heat transfer within the channel.

The average Nusselt number is defined as:

$$Nu = \frac{1}{2A}\int_0^A \left(PruT - \frac{\partial T}{\partial y}\right)_y \mathrm{d}x \qquad (37)$$

where the subscript y denotes the value of the expression within parenthesis at y. We have computed Nu at $y = 0$, the hotter wall and at $y = 0.5$, the middle of the channel.

4. DISCUSSION OF RESULTS

In order to discuss results numerical computations have been performed on taking $A = 1$, $Pr = 7$, $\gamma = 1.4$, $Ec = 0.01$, $\alpha_d = 1.0$ and for different values of Rayleigh number $Ra = 21$, 1000, 14 000 and particle loading $f = 0.0$ and 0.05. The computational results have been presented in Figs. 3–12.

In order to test the grid independency, we have computed the steady-state values of average Nusselt number defined by the equation (37) for the case of clear fluid at the wall and at the middle point of the cavity by taking different grid sizes. The following table shows that there is not significant change in the results due to the increment of grid beyond 40×40 for the case $Ra = 21$.

In order to examine the correctness of the present numerical method, we have first computed the average Nusselt number for the case of clear fluid by taking the dust parameters f, α_d to be zero and compared the results with those computed by Patterson and Imberger [16]. From Fig. 3(a–c), it is clear that our results have complete agreement with those of Patterson and Imberger.

The variation of the velocity components of particle phase along the middle of the channel has been shown in Fig. 4(a, b) for $Ra = 1000$. It is revealed that both the velocity components decrease with increase of mass concentration f. The velocity components attain their maximum values near the wall and at the centre of the channel they are nearly zero. The velocity components for fluid phase are not shown here but their variation with f is not significant. For the same value of Ra, the temperature distribution along the middle of the channel and their change with the change in mass concentration f can be seen when $Ra = 1000$ from Fig. 5(a, b). The distribution of temperature of the particle phase along x-axis is similar to the velocity distribution, i.e. temperature decreases with increase of f, but the distribution along y-axis is not like that. Near wall effect is different from the effect at the middle of the channel.

Figures 6(a–c) and 7(a–c) show the steady state isotherms and stream-lines for clear fluid for $Ra = 21$, 1000, 14 000, respectively. It is seen that for the case of $Ra = 21$ [Fig. 6(a) and 7(a)] the flow is conduction dominated and is very slow. The value of Nusselt number is very close to 1. for larger value of $Ra(=1000)$, i.e. for larger temperature difference between the walls, the flow is convection dominated which is clear from the presence of tilt in the isotherms shown in Fig. 6(b). From Fig. 7(b) for streamlines it is revealed that the velocity of fluid increases with increase of Ra and the circulation is stronger than the previous case. As a result of increased convection unlike the previous case, the isotherms of fluid phase have now become two-dimensional. If we increase the temperature difference further, i.e. the value of $Ra = 14\,000$, Fig. 3(c) shows that Nu_M continually increases to a maximum value 3.72 upto a time 0.027 and, subsequently, decreases slightly to the steady value, i.e. 3.20 at time 0.08, when fluid is free from dust. From Fig. 6(c) we observe that the circulation is stronger for larger Ra. With the increase of circulation the isotherms are found to be more tilted than the previous case. From Fig. 7(c), it is clear that the fluid flow is horizontally parallel in the core region and shows a rapid increase in velocities.

Table 1

Grid size	Nu at $y = 0.0$	Nu at $y = 0.5$
40×40	1.00277	0.997733
60×60	1.00277	0.997741
80×80	1.00278	0.997765

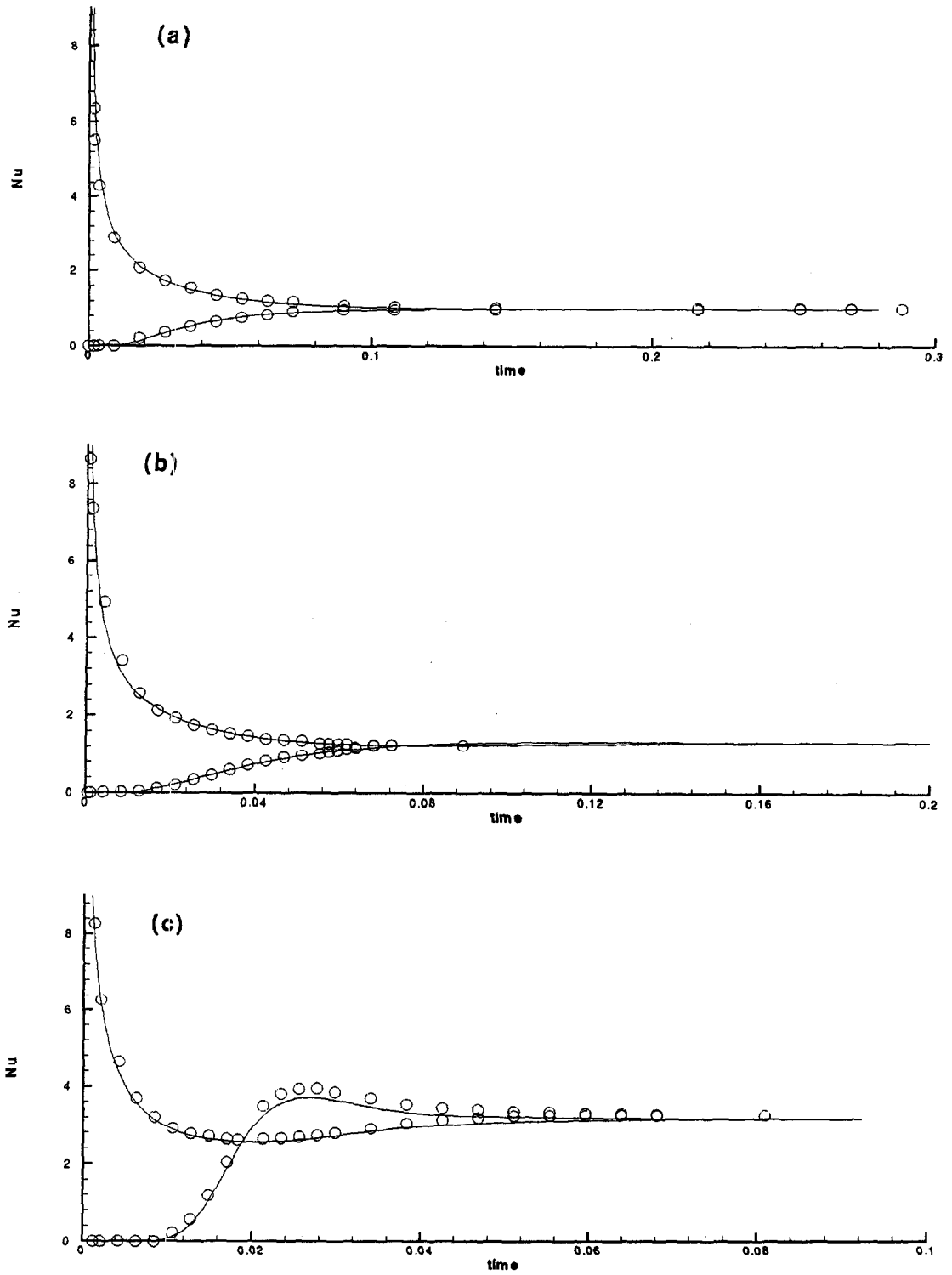

Fig. 3. Comparison of average transient Nusselt number NU_M and NU_W of clear fluid for: (a) $Ra = 21$; (b) $Ra = 1000$; and (c) $Ra = 14000$. ○ results of Patterson and Imberger, — present.

Figures 8(a–c) and 9(a–c) show isotherms of fluid and of particle phase respectively for different values of Ra when mass concentration of particle phase $f = 0.05$. From Fig. 8 it is revealed that there is no significant effect of f on the temperature distribution of fluid in the steady-state condition whereas from Fig. 9 one can easily see that the pattern of isotherms of particle phase are different from that of fluid phase. For the case of particle phase, isotherms are more tilted (one reason may be that the particles are sparsely

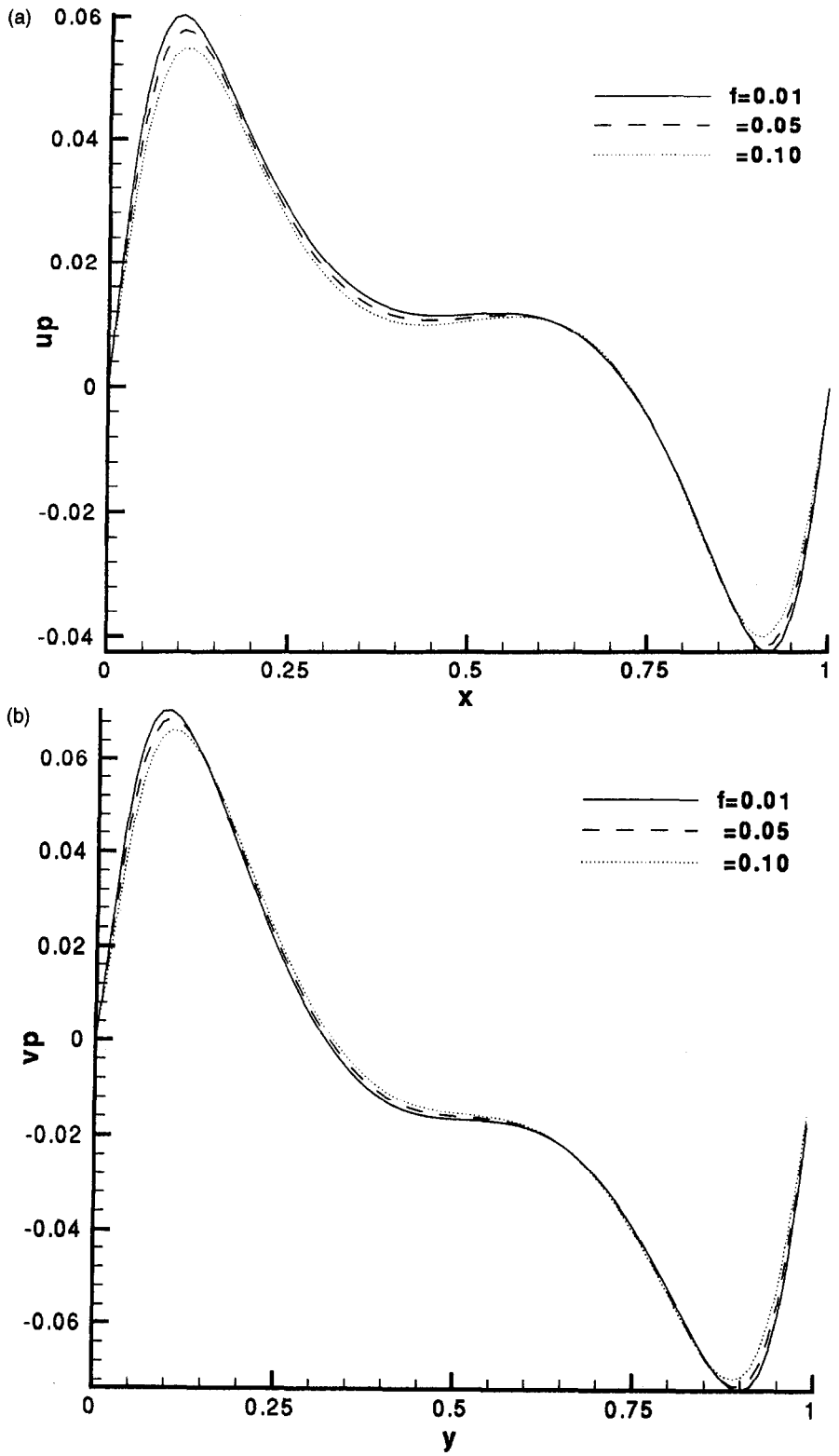

Fig. 4. (a) u_p against x for different values of f when $Ra = 1000$, and $y = 0.5$; (b) v_p against y for different values of f when $Ra = 1000$, and $x = 0.5$.

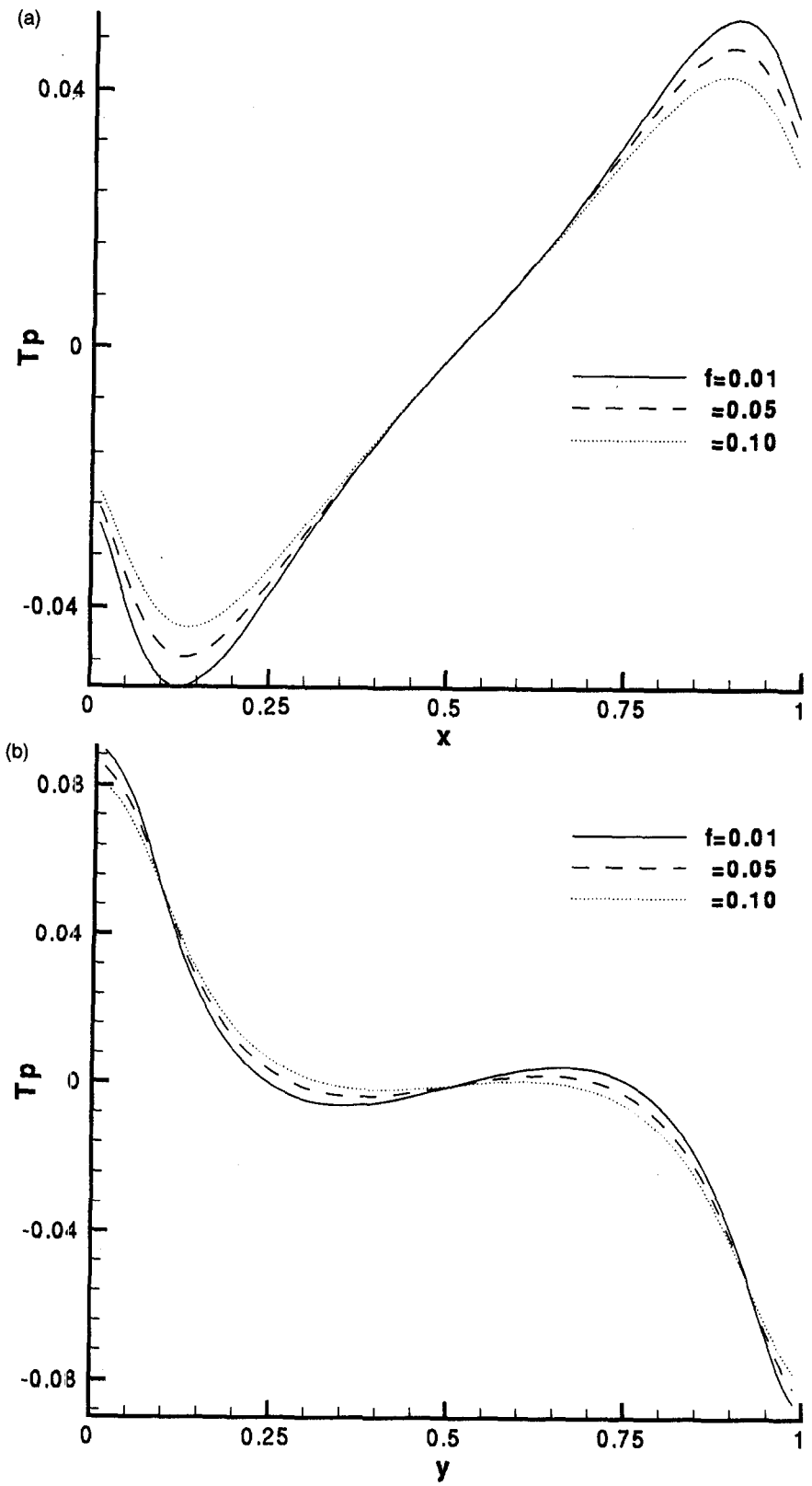

Fig. 5. (a) T_p against x for different values of f when $Ra = 1000$, and $y = 0.5$; (b) T_p against y for different values of f when $Ra = 1000$, and $x = 0.5$.

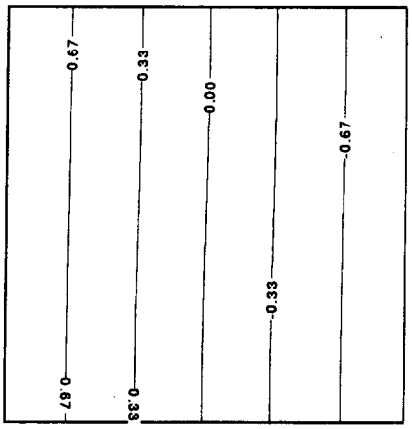

(a)

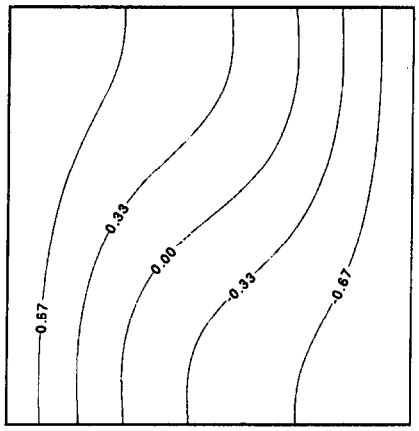

(b)

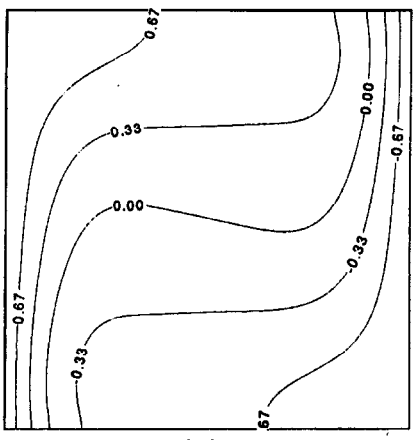

(c)

Fig. 6. Steady-state isotherms of clear fluid for: (a) $Ra = 21$; (b) $Ra = 1000$; and (c) $Ra = 14000$.

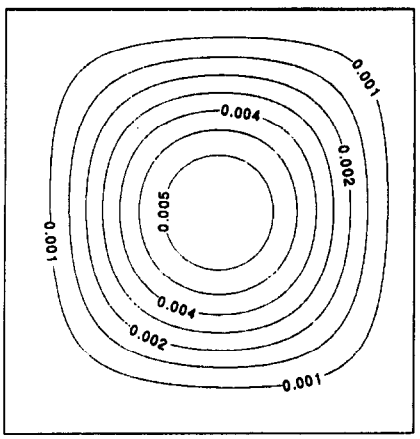

(a)

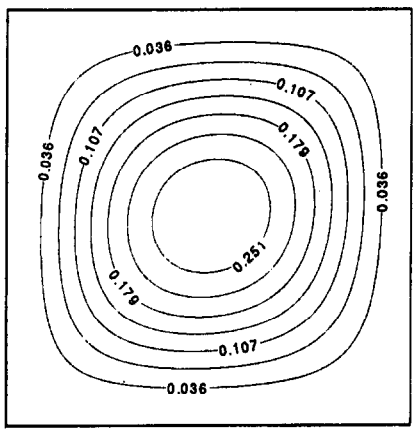

(b)

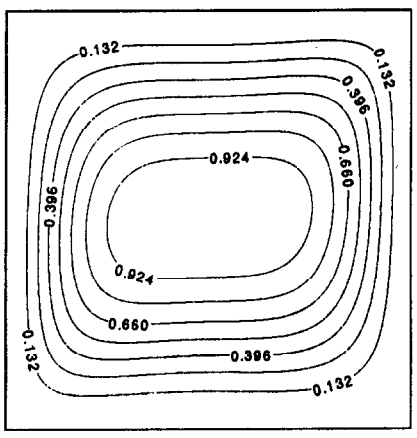

(c)

Fig. 7. Steady-state streamlines of clear fluid for: (a) $Ra = 21$; (b) $Ra = 1000$; and (c) $Ra = 14000$.

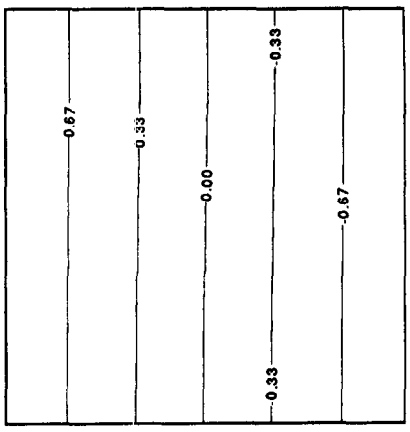

(a)

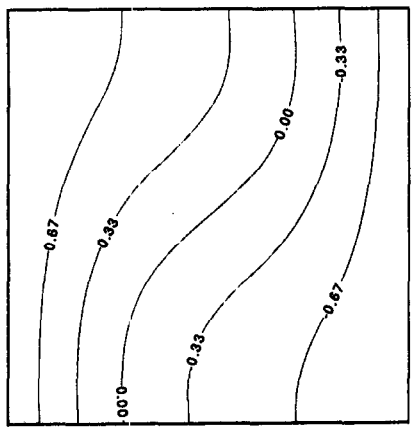

(b)

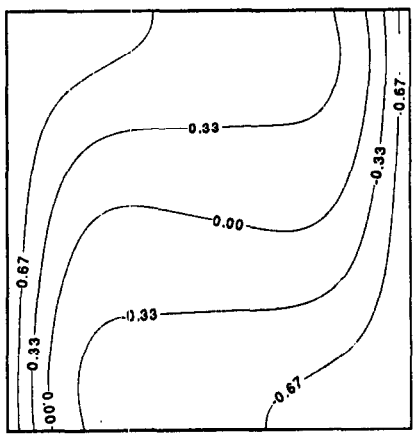

(c)

Fig. 8. Steady-state isotherms of fluid when $f = 0.05$ for: (a) $Ra = 21$; (b) $Ra = 1000$; and (c) $Ra = 14000$.

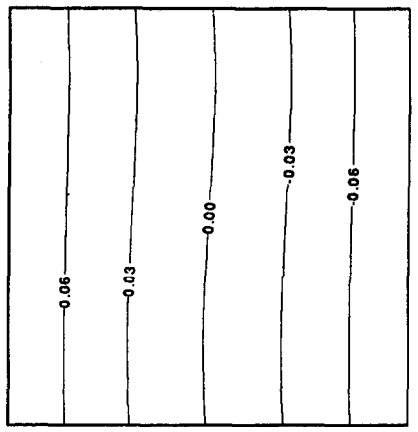

(a)

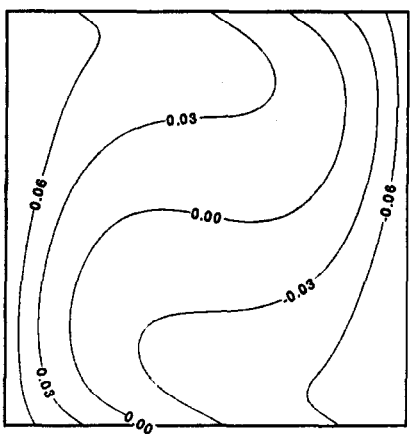

(b)

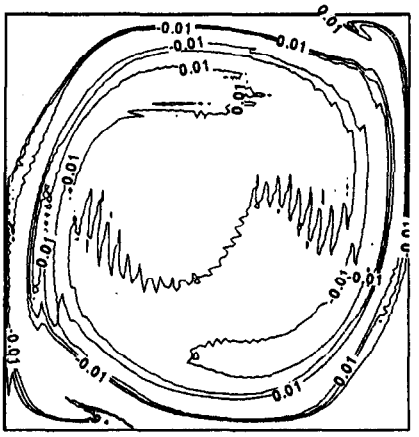

(c)

Fig. 9. Steady-state isotherms of particle phase when $f = 0.05$ for: (a) $Ra = 21$; (b) $Ra = 1000$; and (c) $Ra = 14000$.

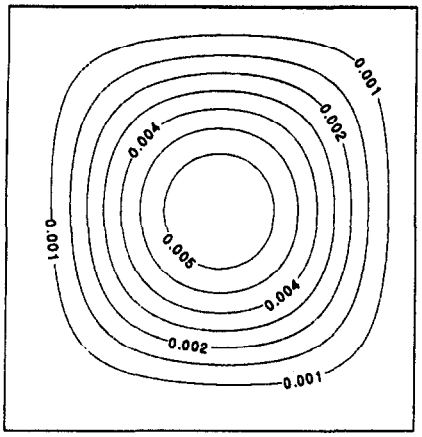

(a)

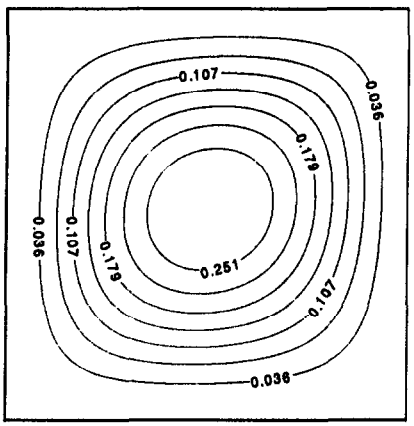

(b)

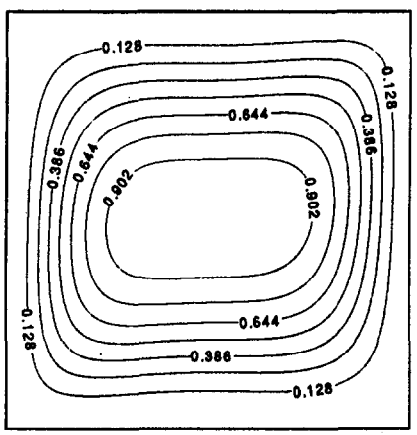

(c)

Fig. 10. Steady-state streamlines of fluid when $f = 0.05$ for: (a) $Ra = 21$; (b) $Ra = 1000$; and (c) $Ra = 14000$.

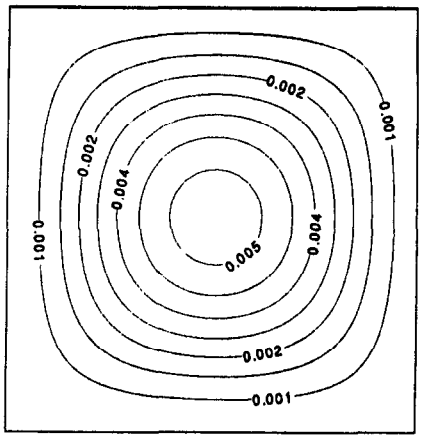

(a)

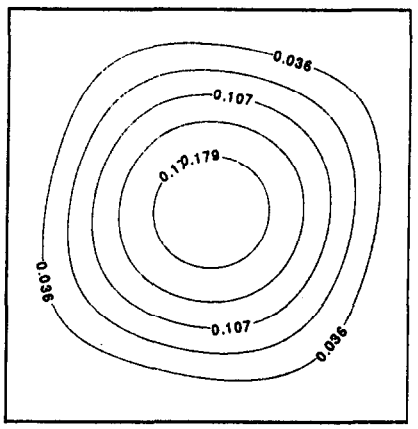

(b)

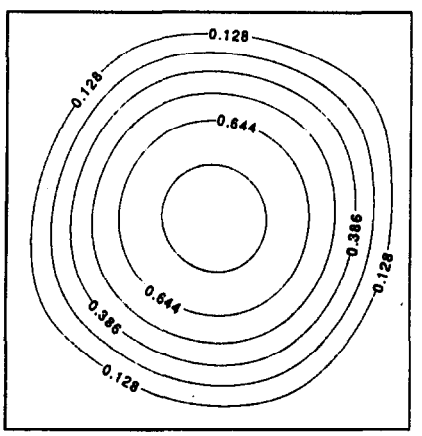

(c)

Fig. 11. Steady-state streamlines of particle phase for: (a) $Ra = 21$; (b) $Ra = 1000$; and (c) $Ra = 14000$.

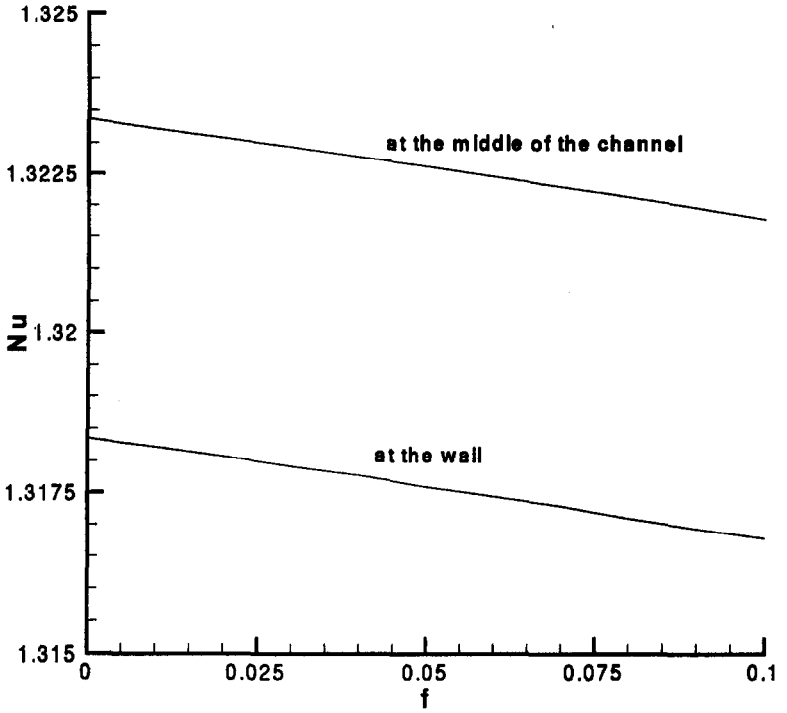

Fig. 12. Steady-state Nusselt number of fluid (Nu) against f when $Ra = 1000$.

distributed and the particle phase is not as continuous as fluid) and the temperature is also less than that of fluid. The streamlines of fluid and of particle phase have been shown in Figs. 10(a–c) and 11(a–c), respectively, for different values of Ra when $f = 0.05$. Figure 10 reveals that the effect of f is not much significant in the velocity of fluid and streamlines are very similar to that of clear fluid. With the increase of Ra, the difference in steady-state stream function values of fluid and particle phase increases and streamlines of fluid become flatter when circulation is stronger, whereas streamlines of particle phase are more of a circular shape and circulation is slower than that of fluid. It can be explained that when velocity of fluid increases with increase of Ra, drag force also increases, which in turn, increase the difference between the velocities of fluid and of particle phase. For $Ra = 14000$, the flow is laminar and slow. The corner vortices have not been found prominent for this value of $Ra = 14000$.

Figure 12 shows the variation in steady-state Nusselt number of fluid with the mass concentration of particle phase. It is seen that Nusselt number of fluid phase decreases with the increase in mass concentration f of particle phase, i.e. heat transfer rate of fluid decreases with increase in mass concentration of particle phase.

5. CONCLUSIONS

Numerical results are reported for the transient heat transfer due to natural convection of a dusty fluid in a finite rectangular channel having adiabatic horizontal walls and differentially heated vertical walls. Computed results have good agreement with the earlier studies [16]. The heat transfer rate of fluid increases with the increase of Rayleigh number and decreases with the increase of mass concentration. The increase of temperature difference between the vertical walls makes the circulation stronger and the difference between stream function values of fluid and particle phase increases. The time to reach steady-state increases with increase of mass concentration.

Acknowledgements—D. C. Dalal would like to thank the Council of Scientific and Industrial Research (CSIR), India for granting the fellowship to pursue the work. We express our deep gratitude to the referees for their valuable suggestions in the improvement of this paper.

REFERENCES

1. Kazakevich, F. P. and Krapivin, A. M., Investigation of heat transfer and of aerodynamical resistance in tube assemblies when the flow of gas is dust-laden. *Izvestiya Vysshikh Uchebnykh Zavedenii Energetika*, 1958, **1**, 101 (in Russian).
2. Saffman, P. G., On the stability of laminar flow of a dusty gas. *Journal of Fluid Mechanics*, 1962, **13**, 120.
3. Marble, F. E., Dynamics of a gas containing small solid particles. *Proceedings of the Fifth AGARD Colloquium Combustion and Propulsion* (1962). Pergamon Press, Oxford, 1963, pp. 175–213.
4. Farbar, L. and Morley, M. J., Heat transfer to flowing gas–solid mixtures in a circular tube. *Industrial Engineering Chemistry*, 1957, **49**, 1143.
5. Farbar, L. and Depew, C. A., Heat transfer effects to gas–solids mixtures using solid spherical particles of uniform size. *I and EC Fundamentals*, 1963, **2**, 130.
6. Sukomel, A. S., Tsvetkov, F. F. and Kerimov, R. V.,

The study of local heat transfer from a tube wall to a turbulent flow of gas bearing suspended solid particles. *Teploenergetika*, 1967, **14,** 77.
7. Tien, C. L. and Quan, V., Local heat characteristics of air–glass and air–lead mixtures in turbulent pipe flow. ASME Paper no. 62-HT-15, 1962.
8. Depew, C. A. and Kramer, T. J., Heat transfer to flowing gas–solid mixtures. *Advances in Heat Transfer*, 1973, **9.**
9. Tien, C. L., Heat transfer by a turbulently flowing fluid–solids mixture in a pipe. *Transactions of ASME, Journal of Heat Transfer*, 1961, **83,** 183.
10. Ramamurthy, V., Free convection effects on the Stokes problem for an infinite vertical plate in a dusty fluid. *Journal of Mathematics and Physics Science*, 1990, **24,** 297.
11. Batchelor, G. K., Heat transfer by free convection across a closed cavity between vertical boundaries at different temperatures. *Quarterly Applied Mathematics*, 1954, **12,** 209.
12. Poots, G., Heat transfer by laminar free convection in enclosed plane gas layers. *Quarterly Journals of Mechanics and Applied Mathematics*, 1958, **11,** 257.
13. Gill, A. E., The boundary-layer regime for convection in a rectangular cavity. *Journal of Fluid Mechanics*, 1966, **26,** 515.
14. Wilkes, J. O. and Churchill, S. W., The finite difference computation of natural convection in a rectangular enclosure. *A.I.Ch.E. Journal*, 1966, **12,** 161.
15. De Vahl Davis, G., Laminar natural convection in an enclosed rectangular cavity. *International Journal of Heat and Mass Transfer*, 1968, **11,** 1675.
16. Patterson, J. and Imberger, J., Unsteady natural convection in a rectangular cavity. *Journal of Fluid Mechanics*, 1980, **100,** 65.
17. Mukherjea, S. K., Study of incompressible separated flow problems in fluid mechanics. Ph.D. thesis, IIT, Kharagpur, India, 1990.
18. Harlow, F. H. and Welch, J. E., Numerical calculation of time dependent viscous incompressible flow of fluid with free surface. *Physics of Fluids*, 1965, **8,** 2182.
19. Hirt, C. W., Nichols, B. D. and Romero, N. C., SOLA—a numerical solution algorithm for transient fluid flows. Los Alamos Scientific Laboratory Report LA-5852, 1975.
20. Harlow, F. H., and Amsden, A. A., Numerical calculation of multiphase fluid flow. *Journal of Computational Physics*, 1975, **17,** 19.
21. Di Giacinto, M., Sabetta, F. and Piva, R., Two-way coupling effects in dilute gas–particle flows. *ASME Journal of Fluids Engineering*, 1982, **104,** 304.
22. Dalal, D. C., Unsteady flow and heat transfer of a dusty fluid. Ph.D. thesis, IIT, Kharagpur, India, 1994.
23. Roache, P. J., *Computational Fluid Dynamics*. Albuquerque, Hermosa, 1972.
24. Jakob, M., Free heat convection through enclosed plane gas layers. *Transactions of the ASME*, 1946, **68,** 189.
25. Mull, W. and Reiher, H., Der Wärmeschutz von Luftschichten. *Beihefte zum Gesumdheits-Ingenieur*, Reihe 1, Heft 28, Germany, 1930.